Reaction Mechanism of Chlorosiloxane Ring Formation from $SiCl_4$ and O_2

Anil Kumar, Thorsten Homann, and Karl Jug*

Theoretische Chemie, Universität Hannover, Am Kleinen Felde 30, 30167 Hannover, Germany

Received: November 15, 2001; In Final Form: April 29, 2002

The formation of the chlorosiloxane ring $(Cl_2SiO)_2$ from the reaction of $SiCl_4$ with O_2 has been studied using density functional theory (DFT). Geometries of reactants, intermediates, transition states, and products were fully optimized, and the relative energies of the stationary points and all of the transition states were calculated on the B3LYP/6-311G* level. The initial reaction of O_2 with $SiCl_4$ starts on the triplet surface with the insertion of O_2 in $SiCl_4$. This will loosen one Cl atom, and a barrier of 56.6 kcal/mol must be overcome. In the next step Cl_2 is eliminated and the cyclic-Cl_2SiO_2 is formed. The latter reacts with $SiCl_4$, which involves a barrier of 76.0 kcal/mol. This process leads to the formation of a low-lying intermediate $Cl_2SiO(OCl)SiCl_3$. The intermediate proceeds under elimination of Cl_2 to the product $(Cl_2SiO)_2$ ring over a barrier of 71.3 kcal/mol. This study also shows that the formation of the Cl_3SiO radical is found to be energetically more favorable than that of Cl_2SiO. This can lead to the growth of larger chlorosiloxanes.

1. Introduction

The reaction of $SiCl_4$ with O_2 is of great technological importance for the chemical vapor deposition (CVD) of solid SiO_2 films used in the microelectronics industry and synthesis of the ceramic powders.[1−6] The basic reaction

$$SiCl_4 + O_2 \rightleftharpoons SiO_2 + 2Cl_2 \quad (1)$$

occurs when the mixture of O_2 with $SiCl_4$, in a tube of about 30 cm length, is heated above 1000 °C.[5,6] However, in the temperature range of 800−1000 °C, the resulting product consists of a multitude of chlorosiloxanes of the general formula $Si_xO_yCl_z$.[6,7] These chlorosiloxanes have a variety of shapes and sizes ranging from chains and rings to oligocyclic and polycyclic shapes. A large number of chlorosiloxanes were identified by mass spectrometry.[6−11] These chlorosiloxanes are intermediate compounds formed in the course of the reaction because of the partial replacement of Cl atoms in $SiCl_4$ by oxygen atoms.

Actually, the chemical kinetics mechanism of the SiR_4 (R = H or Cl) combustion is complex and not fully understood, and generally, it is proposed that the first step of the reaction occurs because of the formation of SiR_3 radical, which further reacts with O_2 to give the SiR_3OO adduct:[12,13]

$$SiR_4 \rightleftharpoons SiR_3 + R \quad (2)$$

$$SiR_3 + O_2 \rightleftharpoons SiR_3OO \quad (3)$$

Powers[14] and French et al.[15] measured the decomposition reaction of $SiCl_4$ into $SiCl_3 + Cl$ between 1100 and 1300 °C and estimated the activation barrier of 96 kcal/mol and suggested the following reaction with oxygen:

$$SiCl_4 + O_2 \rightleftharpoons SiCl_3OO + Cl \quad (4)$$

On the basis of this mechanism, several groups attempted to understand the oxidation of SiR_4 using both theory and experiment.[16−20] Niiranen and Gutman[16] studied the gas-phase kinetics of the reactions of two substituted silyl radicals, $Si(CH_3)_3$ and $SiCl_3$, with O_2 as a function of temperature by using a heated tubular reactor coupled to a photoionization mass spectrometer to identify the products of the reaction. Tezaki et al.[17] studied the dissociation of $SiCl_4$ using laser pulses and observed the formation of SiCl, $SiCl_2$, and $Si(^3P)$. They observed that Si and SiCl react rapidly with O_2 in comparison to $SiCl_2$, while SiO was detected as the primary product of the initial oxidation process. Koshi et al.[18] identified the presence of the SiH_3O radical as a direct product of the $SiH_3 + O_2$ reaction at ambient temperature using time-resolved mass spectrometry.

Darling and Schlegel[19] studied the $SiH_3 + O_2$ reaction using ab initio G2 level of theory and found the formation of H_2SiOOH via 1,3-hydrogen shift from H_3SiOO involving a transition state. Murakami et al.[20] performed ab initio G2 level calculations to study the reaction $SiH_3 + O_2$ for the production of SiO. They found a transition state for the production of cyclic-H_2SiO_2 (siladioxirane) from the SiH_3OO adduct. These studies were limited to the understanding of the mechanism of SiO formation considering unimolecular decomposition of the SiH_3OO adduct. No attention was given to the formation of siloxanes, which are produced as intermediate compounds during the combustion reaction of SiR_4 with O_2. Using IR absorption spectroscopy, Wood et al.[21] succeeded in identifying the formation of chlorosiloxanes in the reaction of a $SiCl_4/O_2$ mixture at elevated temperature. Between 900 and 1100 °C, they were able to detect the formation of silicon oxychlorides, such as Si_2OCl_6 and cyclic-$Si_4O_4Cl_8$, whereas Kornick and Binnewies successfully proved the presence of larger chlorosiloxane molecules.[22]

Recently, Junker et al.[23] found the presence of highly reactive species $SiOCl_2$ during combustion of $SiCl_4$ with O_2. They proposed that the presence of $SiOCl_2$ can lead to the formation of chlorosiloxanes.

With the availability of $SiOCl_2$, one could imagine that the following reactions lead to the chlorosiloxane chain and ring formation:

$$SiOCl_2 + SiCl_4 \rightleftharpoons Si_2OCl_6 \quad (5)$$

$$2SiOCl_2 \rightleftharpoons Si_2O_2Cl_4 \quad (6)$$

10.1021/jp014235o CCC: $22.00
Published on Web 06/26/2002

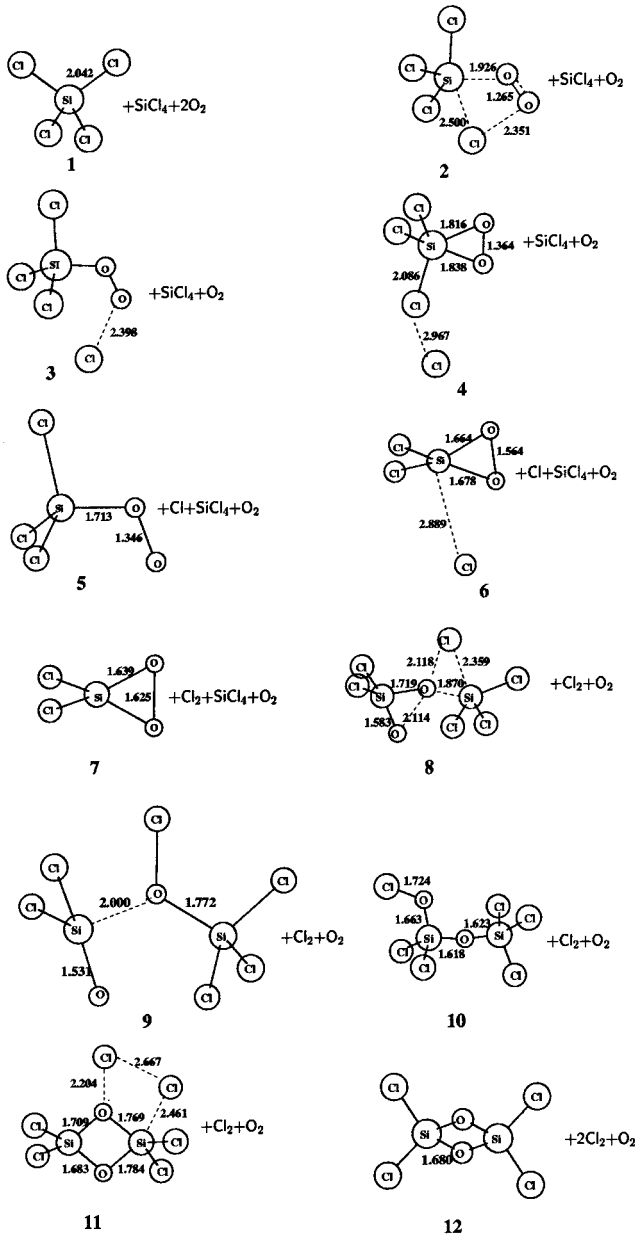

Figure 1. Structural parameters (Å) of reactants, intermediates, transition states, and products appearing in pathway A, optimized at the B3LYP/6-311G* level.

Wilkening and Binnewies[24] proposed the formation of higher condensed siloxanes via $SiCl_4$ elimination. However, they could not identify the presence of $SiOCl_2$ using a mass spectrometer. They detected its formation with matrix IR spectroscopy.[23] They further performed DFT calculations to compare the thermochemical properties of $SiOCl_2$. In another recent study, higher chlorosiloxanes were formed by the thermolysis of Si_2OCl_6 and involvement of $SiOCl_2$ has been emphasized for the larger chlorosiloxane growth.[24]

Quite recently, Jug and Wichmann extensively carried out semiempirical calculations on a variety of chlorosiloxanes.[6,25−29] First, they studied the structure and stability of different chlorosiloxanes building units, considering chains and monocyclic rings.[25,26] On the basis of their theoretical studies, they also proposed a growth mechanism for the formation of larger hydridosilsequioxanes by introducing an elementary building unit, $Si_2O_3H_2$.[27] In a subsequent study, they demonstrated the tubelike shape of large silsesquioxanes, $Si_{2n}O_{3n}H_{2n}$, with n up to 120 and proposed that these structures can be considered as prestages of nanotubes.[28] Using the ab initio MP2/6-311+G(d) method, they studied the decomposition reaction of perchlorodisiloxane to understand the growth of chlorosiloxane molecules considering various possible reaction pathways.[29]

Thus, our primary objective in this present study is to explore the reaction mechanism of chlorosiloxane ring formation from the basic reaction of $SiCl_4$ and O_2

$$2SiCl_4 + O_2 \rightleftharpoons (Cl_2SiO)_2 + 2Cl_2 \qquad (7)$$

TABLE 1: Vibrational Frequencies (cm^{-1}) of Transition States[a] Calculated at B3LYP/6-311G* Level

structures	frequencies
2	*i*152, 35, 114, 155, 193, 220, 236, 246, 304, 323, 466, 482, 521, 607, 1235
4	*i*146, 26, 42, 93, 166, 182, 225, 237, 249, 293, 418, 532, 612, 648, 1153
6	*i*154, 77, 128, 197, 215, 241, 250, 443, 582, 635, 729, 1000
8	*i*194, 26, 28, 68, 78, 120, 150, 160, 211, 218, 221, 226, 264, 265, 307, 334, 371, 459, 512, 528, 609, 630, 708, 1079
11	*i*358, 10, 46, 53, 101, 130, 151, 158, 181, 199, 221, 239, 267, 287, 339, 370, 479, 600, 612, 618, 656, 729, 781, 952
16	*i*412, 106, 214, 264, 388, 1661
19	*i*319, 3, 23, 76, 91, 128, 144, 151, 165, 174, 209, 215, 252, 263, 285, 335, 359, 470, 575, 621, 626, 640, 824, 919
20	*i*155, 30, 55, 80, 93, 125, 142, 161, 186, 199, 209, 236, 255, 276, 382, 422, 454, 592, 613, 619, 620, 643, 771, 1115
23	*i*317, 27, 47, 58, 76, 95, 103, 118, 131, 131, 161, 197, 219, 232, 246, 260, 299, 333, 469, 479, 587, 587, 1124, 1144

[a] See Figures 1 and 2.

TABLE 2: Mechanistic Steps and Calculated Relative Energies (kcal/mol) of Reactants, Transition States, Intermediates, and Products

structures	reaction	mechanistic step	energy
1	$2SiCl_4 + 2O_2$	O_2 triplet	0.0
1′[a]	$2SiCl_4 + 2O_2$	O_2 singlet	39.0
2	$Cl_4SiO_2 + SiCl_4 + O_2$	O_2 insertion	56.6
2′[a]	$Cl_4SiO_2 + SiCl_4 + O_2$	O_2 insertion	74.5
3	$Cl_3SiO_2Cl + SiCl_4 + O_2$	Cl loosening	48.1
3′[a]	$Cl_3SiO_2Cl + SiCl_4 + O_2$	Cl loosening	29.4
4	$Cl_2SiO_2Cl_2 + SiCl_4 + O_2$	Cl_2 abstraction	63.7
4′[a]	$Cl_2SiO_2Cl_2 + SiCl_4 + O_2$	Cl_2 abstraction	91.6
5	$Cl_3SiO_2 + Cl + SiCl_4 + O_2$	Cl abstraction	55.3
6	$Cl_2SiO_2Cl + Cl + SiCl_4 + O_2$	Cl loosening	99.5
7	$Cl_2SiO_2 + Cl_2 + SiCl_4 + O_2$	Cl_2 formation	56.0
8	$Cl_2SiO_2SiCl_4 + Cl_2 + O_2$	$SiCl_4$ addition	76.0
9	$Cl_2SiO(OCl)SiCl_3 + Cl_2 + O_2$	Cl migration	50.6
10	$Cl_2SiO(OCl)SiCl_3 + Cl_2 + O_2$	$SiCl_3$ migration	−12.9
11	$Cl_2SiO(OCl)SiCl_3 + Cl_2 + O_2$	Cl_2 elimination	58.4
12	$(Cl_2SiO)_2 + 2Cl_2 + O_2$	ring formation	−2.1
13	$Cl_3SiO + OCl + SiCl_4 + O_2$	OCl abstraction	59.5
14	$(Cl_3SiO)_2 + O_2Cl_2$	O_2Cl_2 formation	50.9
15	$(Cl_3SiO)_2 + O_2Cl + Cl$	Cl abstraction	59.6
16	$(Cl_3SiO)_2 + O_2Cl_2$	Cl_2 elimination	92.8
17	$(Cl_3SiO)_2 + O_2 + 2Cl$	Cl abstraction	64.2
18	$(Cl_3SiO)_2 + Cl_2 + O_2$	Cl_2 formation	18.2
19	$Cl_2SiO(OCl)SiCl_3 + Cl_2 + O_2$	Cl loosening	72.7
20	$(Cl_3SiO)_2 + Cl_2 + O_2$	Cl_3SiO rotation	34.6
21	$2Cl_3SiO + Cl_2 + O_2$	Cl_3SiO fragmentation	61.6
22	$2Cl_2SiO + 2Cl + O_2 + Cl_2$	$SiOCl_2$ formation	104.8
23	$(Cl_3SiO)_2 + Cl_2 + O_2$	Cl_2 elimination	116.9
24	$SiCl_3 + Cl + SiCl_4 + 2O_2$	$SiCl_3$ formation	95.7

[a] Corresponds to the alternative reaction pathways (see Figures 3−5).

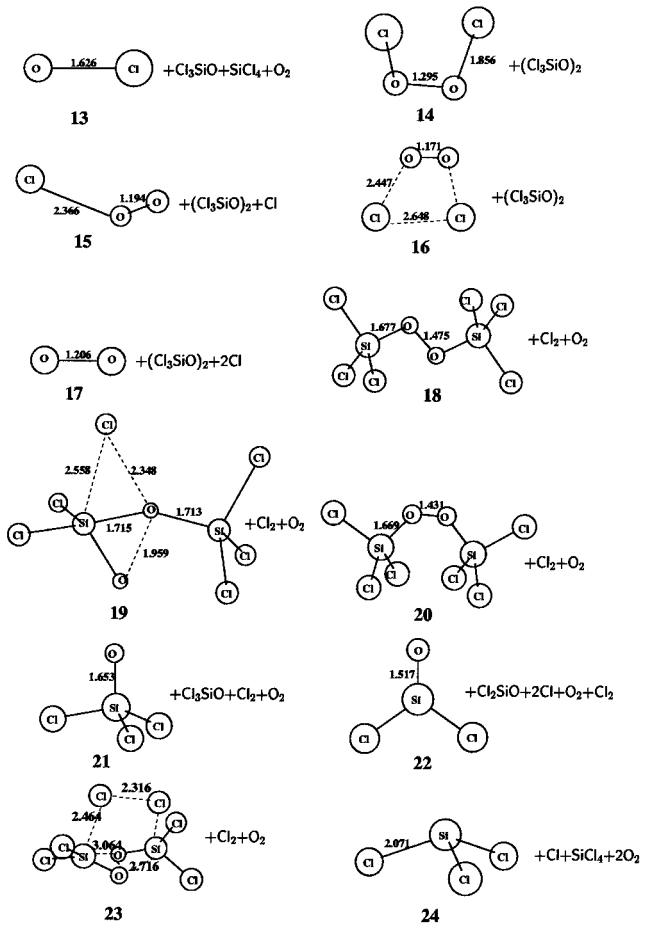

Figure 2. Structural parameters (Å) of reactants, intermediates, transition states, and products appearing in pathways B and C, optimized at the B3LYP/6-311G* level.

considering different pathways: (i) direct insertion of O_2 in $SiCl_4$, (ii) decomposition of the $SiCl_3OOCl$ adduct into $SiCl_3O$ + OCl, produced in step i, and (iii) decomposition of $SiCl_4$ into $SiCl_3$ + Cl and its further reaction with O_2.

2. Computational Details

Molecular orbital calculations were carried out using the Gaussian 94[30] series of programs to study the ground-state reaction. In the present study, we use the density functional theory (DFT) of Becke's three-parameter hybrid functional[31] combined with the Lee−Yang−Parr correlation functional (B3LYP).[32] Among different methods, the B3LYP method has been found to be most accurate and computationally economic in its performance on the G2 molecule set using different basis sets.[33] For economic reasons, we used the 6-311G* basis set for the optimization of the geometries of the reactants, intermediates, transition states, and products. Vibrational frequency calculations using analytical second derivatives were performed for all of the stable molecules and transition states to verify the nature of the stationary points located on the potential energy surface. For transition states, the existence of only one imaginary frequency was checked. To ensure that the transition state joins the two intermediates on the potential energy surface, an intrinsic reaction coordinate (IRC)[34] analysis was also performed using the B3LYP/6-311G* level.

3. Results and Discussion

The structures of the reactants, intermediates, transition states, and products, optimized on the B3LYP/6-311G* level, are given in Figures 1 and 2. Energy level diagrams for three reaction mechanisms are shown in Figures 3, 4, and 5. The relative energies, calculated with respect to the reactants, are given in kilocalories per mole, and the bold numbers correspond to the respective structure given in Figures 1 and 2. A reaction scheme leading from reactant to product involving different species is shown in Figure 6. In Figure 6, we connected structures in the sequence in which they are passing through the reaction paths. The structures are numbered as bold and their types are reactant, intermediate, transition state, or two radicals. The vibrational frequencies of transition states, calculated using B3LYP/6-311G* level, are presented in Table 1. The relative energies of reactants, transition states, intermediates, products, and the mechanistic reaction steps are given in Table 2. Total energies, zero-point energies (ZPE), and thermal correction of the species involved in the reaction are given in Table 3. The ZPE and thermal correction refer to the species listed under molecule at room temperature. The sum of the thermal corrections of all species listed as reactants, intermediates, transition states, and products in Table 2 and Figures 1 and 2 varies between 27.0 (**13**) and 30.8 kcal/mol (**1**). Because this variation is small, these corrections have no influence on the mechanism and are not included in the relative energies in Figures 3−5. For the few selected compounds **1** ($SiCl_4$), **17** (O_2), **8** ($ClSiO_2SiCl_4$), **19** ($ClSiO(OCl)SiCl_3$), and Cl_2, thermal corrections were also calculated at 1200 K, that is, in the temperature range of the experiments. They suggest that the thermal corrections are not essential for the reaction mechanism.

TABLE 3: Total Energies (au)[a], Zero-Point Energies (ZPE), and Thermal Correction (kcal/mol) for the Species Involved in the Reaction, Calculated Using B3LYP/6-311G* Level

structures	molecule	total energy	ZPE	thermal[b]
1	$SiCl_4$	−2130.604 621	4.5	8.6
2	Cl_4SiO_2	−2280.879 163	7.3	12.9
3	Cl_3SiO_2Cl	−2280.892 820	7.6	13.7
4	$Cl_2SiO_2Cl_2$	−2280.867 783	7.0	12.8
5	Cl_3SiO_2	−1820.715 187	7.1	11.8
6	Cl_2SiO_2Cl	−1820.644 650	6.4	10.9
7	Cl_2SiO_2	−1360.474 533	6.4	9.9
8	$Cl_2SiO_2SiCl_4$	−3491.047 024	10.8	19.3
9	$Cl_2SiO(OCl)SiCl_3$	−3491.085 365	11.3	20.2
10	$Cl_2SiO(OCl)SiCl_3$	−3491.188 866	12.4	21.0
11	$Cl_2SiO(OCl)SiCl_3$	−3491.075 238	11.7	19.8
12	$(Cl_2SiO)_2$	−2570.765 933	11.3	17.2
13	OCl	−535.339 425	1.13	2.6
14	O_2Cl_2	−1070.718 302	4.1	7.0
15	O_2Cl	−610.538 239	2.9	5.4
16	O_2Cl_2	−1070.651 619	3.8	6.8
17	O_2	−150.364 785	2.3	3.8
18	$(Cl_3SiO)_2$	−3491.139 361	12.1	20.7
19	$Cl_2SiO(OCl)SiCl_3$	−3491.052 491	10.8	19.3
20	$(Cl_3SiO)_2$	−3491.113 189	11.8	19.9
21	Cl_3SiO	−1745.535 092	5.0	9.0
22	Cl_2SiO	−1285.300 138	4.4	7.4
23	$(Cl_3SiO)_2$	−3490.981 989	10.2	19.3
24	$SiCl_3$	−1670.286 028	3.0	6.3
	Cl_2	−920.405 712	0.7	2.3
	Cl	−460.166 160	0.0	0.9

[a] 1 au = 627.51 kcal/mol. [b] Standard 298.15 K.

3.1. Pathway A. The minimum energy path of the initial reaction of $SiCl_4$ with O_2 starts with the insertion of O_2 by loosening one of the Si−Cl bonds of $SiCl_4$ and involves a triplet transition structure (TS) **2** shown in Figure 1. The barrier height calculated from the reactant **1** in the triplet state is 56.6 kcal/mol (Figure 3). The calculated Si−Cl bond length of 2.042 Å in $SiCl_4$ is in close agreement with the experimental value, 2.030 Å.[35] For UMP2/6-311G(d,p)[36] and local spin density approximation (LSDA),[37] the calculated value is 2.020 and 2.017

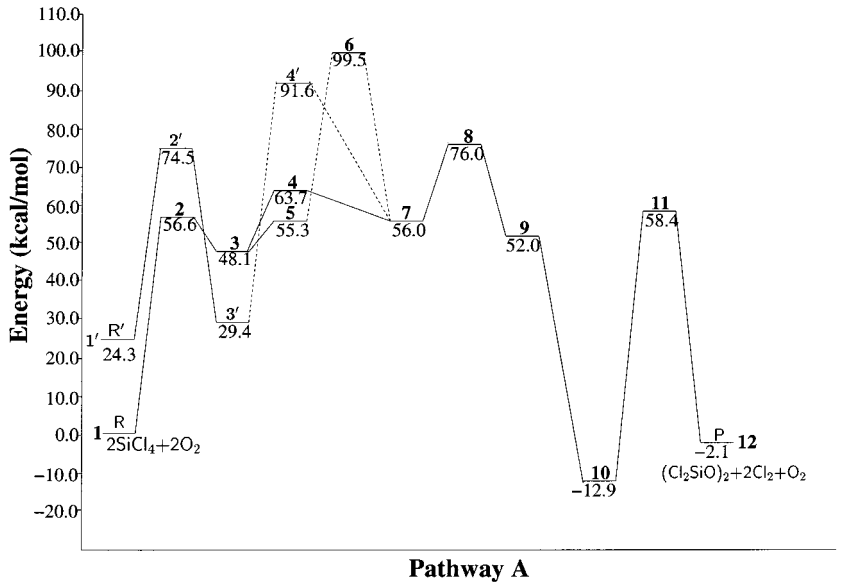

Figure 3. Energy profile (kcal/mol) of $SiCl_4 + O_2$ reaction along pathway A, calculated at the B3LYP/6-311G* level. Bold numbers correspond to structures in Figure 1.

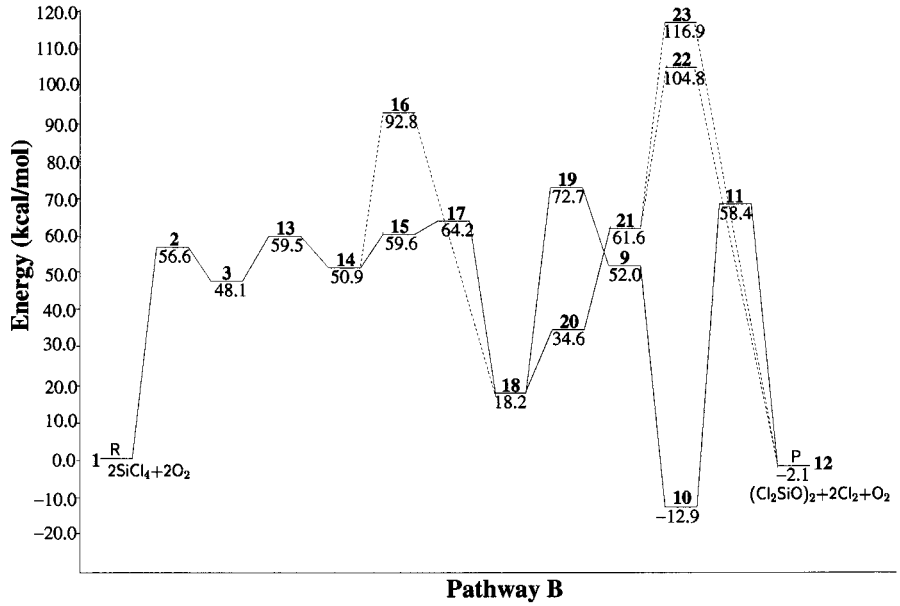

Figure 4. Energy profile (kcal/mol) of $SiCl_4 + O_2$ reaction along pathway B, calculated at the B3LYP/6-311G* level. Bold numbers correspond to structures in Figures 1 and 2.

Å, respectively, and shows a larger deviation from experiment. We found that in the transition state (**2**) oxygen starts bond forming with Si, thereby weakening one of the Si−Cl bonds. The corresponding bond lengths of 1.926 and 2.500 Å are shown in Figure 1. Further, intrinsic reaction coordinate (IRC) analysis, in forward and backward direction from TS (considering 20 points in each direction), confirms that the corresponding transition state **2** links the reactants ($SiCl_4 + O_2$) and the intermediate, Cl_3SiO_2Cl (**3**), in the triplet state (Figures 1 and 3). Geometry optimization of Cl_3SiO_2Cl (**3**) in the triplet state shows that the Cl atom is weakly complexing with the Cl_3SiO_2 moiety, having the distances 3.679 and 2.398 Å from Si and O atoms, respectively (Figure 1). This intermediate **3** lies 48.1 kcal/mol higher with respect to the reactant **1** as shown in Figure 3. From this intermediate **3**, we considered the two alternative pathways for the reaction to proceed further: (i) dissociation of a Cl atom from Cl_3SiO_2Cl (**3**), which leads to the formation of Cl_3SiO_2 intermediate (**5**) and Cl, which lies 55.3 kcal/mol higher than reactant **1** and 7.2 kcal/mol higher than intermediate **3** (Figure 3) via a negligible barrier of less than 1 kcal/mol, and (ii) elimination of Cl_2 from Cl_3SiO_2Cl (**3**), which leads to the formation of Cl_2SiO_2 (**7**) and Cl_2, involving a transition structure **4** in the triplet state, which lies 63.7 kcal/mol above reactant **1** and 15.6 kcal/mol above **3**. The transition structure **4** (Figure 1) shows that one of the Si−Cl bonds is slightly elongated to 2.086 Å so that there is an increased possibility for Cl−Cl bonding compared to intermediate **3**. More important, the second oxygen atom starts bonding to the Si atom.

We also considered the insertion of singlet O_2 with $SiCl_4$. The energy of the respective state, R′ (**1′**) (Figure 3), lies 24.3 kcal/mol above the energy in the triplet state R (**1**). This difference represents the singlet−triplet splitting of O_2 and compares favorably with the experimental value of 22.5 kcal/mol.[38] The singlet of O_2 was calculated with the UB3LYP procedure, which is superior to the B3LYP because the latter refers to a single determinant and therefore represents a mixture

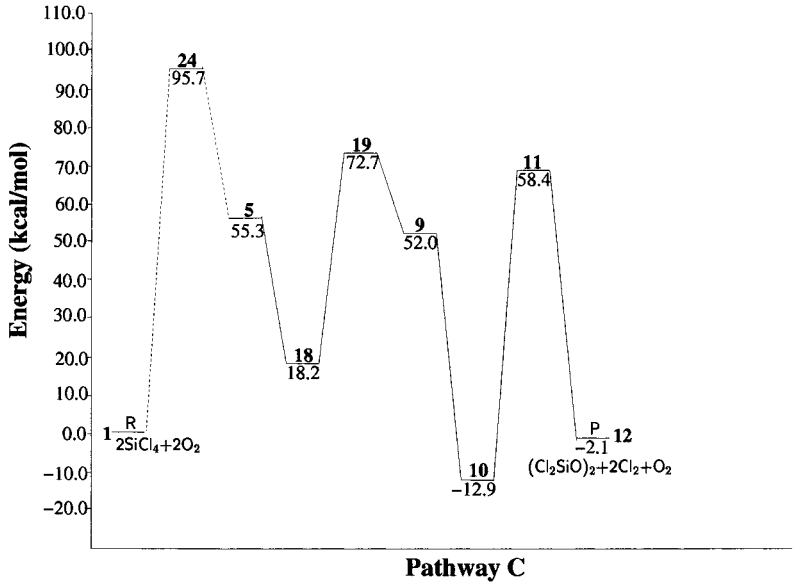

Figure 5. Energy profile (kcal/mol) of $SiCl_4 + O_2$ reaction along pathway C, calculated at the B3LYP/6-311G* level. Bold numbers correspond to structures in Figures 1 and 2.

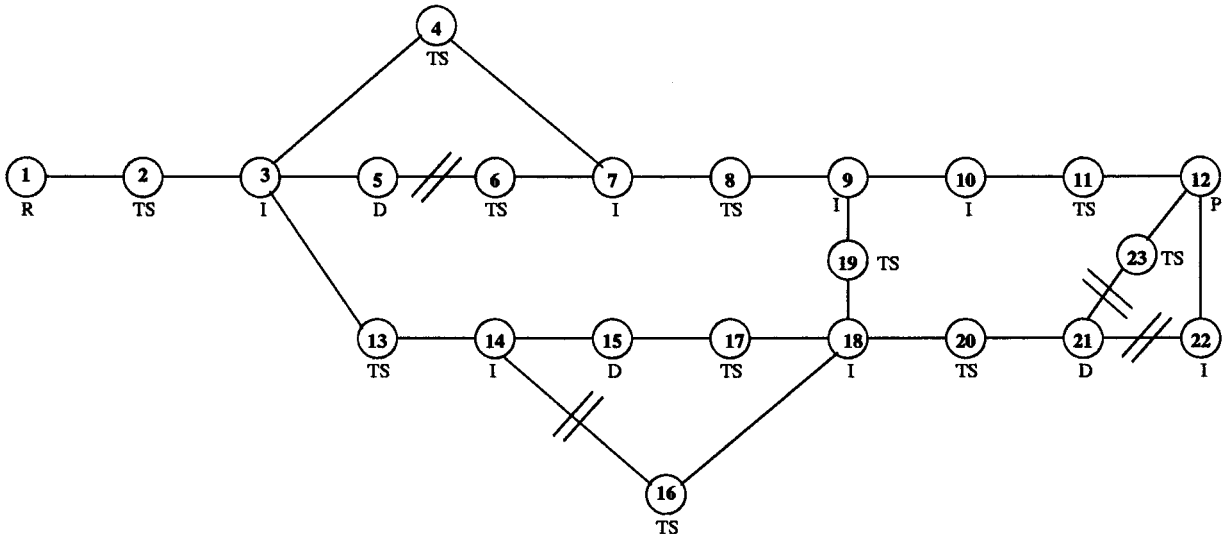

Figure 6. Reaction scheme for pathways A and B of Figures 3 and 4 with reactant (R), intermediates (I), transition states (TS), radicals (D), and product (P).

of Δ_g and $\sum_g^+$. The insertion of O_2 in $SiCl_4$ follows the same mechanism as found in the triplet state. The singlet transition state **2′** (structure not shown) lies at 74.5 kcal/mol with respect to the reactant R (**1**). This transition state **2′** connects the reactant R′ (**1′**) and the intermediate Cl_3SiO_2Cl (**3′**) (Figure 3). The intermediate Cl_3SiO_2Cl (**3′**) is found to be 18.7 kcal/mol more stable than **3** in the triplet state. Here, we found the crossing of singlet and triplet state. Also, a slight difference in structure of the intermediate Cl_3SiO_2Cl in singlet (**3′**) and triplet (**3**) states has been found, that is, the detached Cl atom in the singlet state joined with one of the oxygen atoms with an O−Cl bond length of 1.749 Å, while it is weakly complexing with the Cl_3SiO_2 moiety in the triplet state **3**.

The elimination of Cl_2 from Cl_3SiO_2Cl (**3′**) leads to the formation of Cl_2SiO_2 (**7**), which proceeds through a transition state **4′** (Figure 3). This has a relatively high barrier of 91.6 kcal/mol with respect to the reactant **1**. Here, we again found that the singlet state **4′** crosses the triplet surface **4**, and it seems that at this stage the reaction proceeds on the triplet surface, which further stabilizes on the singlet surface with the formation of Cl_2SiO_2 (**7**) and Cl_2 (Figures 1 and 3). However, the breaking of Cl from doublet Cl_3SiO_2 (**5**) to form singlet Cl_2SiO_2 (**7**) and Cl involves a transition state **6** with an energy of 99.5 kcal/mol relative to the reactant **1** and of 44.2 kcal/mol with respect to **5** (Figure 3).

Using MP2(full)/6-31G(d,p) and G2(MP2) level of theories, Murakami et al.[20] studied the reaction $SiH_3 + O_2$ to identify the possible products that lead to the formation of SiO. They concluded that cyclic-SiH_2O_2(siladioxirane) and H atom is formed from the SiH_3OO adduct through the involvement of a transition state. They found the transition state in C_1 symmetry having pyramidalized siladioxirane structure with one elongated Si−H bond. They calculated the barrier height at 31.5 kcal/mol relative to the SiH_3OO at the G2(MP2) level.[20] Our B3LYP/6-311G* calculated transition state **6**, too, has one elongated Si−Cl bond and a pyramidalized structure in C_1 symmetry. However, Darling and Schlegel,[19] proposed the isomerization of SiH_3OO to SiH_2OOH as the lowest energy pathway for the unimolecular decomposition of SiH_3OO into SiH_2O and OH. The barrier heights of the transition state calculated by Mu-

rakami et al.[20] and Darling and Schlegel[19] were found to be 34.2 and 35.2 kcal/mol with respect to SiH_3OO. Kondo et al.[39] performed ab initio G2 calculations to explore the reaction mechanism of $SiH_3 + O_2$, and they also proposed the formation of a cyclic-$OSiH_2O$ with a barrier height of 29.3 kcal/mol with respect to SiH_3OO. The cyclic-$OSiH_2O$ closely resembles the structure of the cyclic-SiH_2O_2 (siladioxirane)[20] and is found to be 1.11 kcal/mol higher in energy than cyclic-SiH_2O_2. If we, also, consider the same mechanism for the unimolecular decomposition of Cl_3SiO_2 (**5**) into Cl_2SiO and OCl, the barrier height is 47.5 kcal/mol, calculated as the energy difference between reactant and product (see Table 3), with respect to Cl_3SiO_2 (**5**). Thus, this pathway is not feasible in our reaction scheme for the formation of Cl_2SiO; however, the formation of cyclic-Cl_2SiO_2 (**7**) in our calculation follows the minimum energy path as found by Murakami et al.[20] and Kondo et al.[39] Formation of Cl_2SiO_2 from the reaction of $SiCl_2$ with O_2 has been proposed because of the high rate constant of the reaction.[40]

From Cl_2SiO_2 (**7**), there are two possible pathways, both on the singlet potential surface: (i) the unimolecular decomposition of Cl_2SiO_2 (**7**) for the formation of SiO and (ii) the bimolecular reaction of Cl_2SiO_2 with $SiCl_4$ for the chlorosiloxane ring $(Cl_2SiO)_2$ formation. The first possibility has been widely considered to understand the formation of SiO from the reaction $SiH_3 + O_2$.[19,20,39] In our study, we considered the second pathway and found that Cl_2SiO_2 (**7**) further reacts with $SiCl_4$ with a migration of a Cl atom from $SiCl_4$ to one of the oxygen atoms of Cl_2SiO_2 (**7**) involving a transition state **8**, which lies 76.0 kcal/mol higher than reactant **1**. We have repeated the calculation of this barrier with the larger 6-311+G(2df) basis set. The relative energy of structure **8** to structure **1** changed to 77.8 kcal/mol, which is an insignificant change. We considered this reaction in the singlet state. The transition state **8**, shown in Figure 1, shows that one Si−Cl bond of $SiCl_4$ is elongated to 2.359 Å and one of the oxygen atoms of Cl_2SiO_2 (**7**) begins to bind with Si of $SiCl_4$ with a bond length of 1.870 Å. Also, the O−O bond of Cl_2SiO_2 (**7**) is found to be broken (2.114 Å). One Si−O bond of Cl_2SiO_2 (**7**) becomes shorter (1.583 Å) showing some double-bond character and the corresponding bond length with the second oxygen atom becomes longer 1.719 Å (Figure 1). We did an IRC analysis, which shows that the corresponding transition state **8** connects the two intermediates (Cl_2SiO_2 (**7**) + $SiCl_4$) and $Cl_2SiO(OCl)SiCl_3$ (**9**) (Figures 1 and 3). According to the IRC analysis, we further fully optimized the structure of the intermediate $Cl_2SiO(OCl)SiCl_3$ (**9**), but we found this intermediate to be unstable on the potential energy surface. It transforms to the intermediate **10** (Figures 1 and 3). The intermediate **10** differs from **9** in the different location of the $SiCl_3$ unit, as shown in Figure 1. To resolve this ambiguity, we scanned the potential energy surface by changing the distance between O and Si of the $SiCl_3$ unit in **9** from 3.2 to 3.6 Å with the step size of 0.1 Å and located the minimum at 3.400 Å (shown in Figure 1) and calculated a very low barrier, about 0.9 kcal/mol, separating the two intermediates **9** and **10**. This low barrier can be easily overcome even at low temperature. The intermediate **10** is found to be more stable by −12.9 kcal/mol with respect to the reactant **1**. Further, the elimination of the Cl_2 from this intermediate $Cl_2SiO(OCl)SiCl_3$ (**10**) leads to the formation of the desired product $(Cl_2SiO)_2$ (**12**) and Cl_2. It proceeds via a transition state **11**, which lies 58.4 kcal/mol above the reactants **1** and 71.3 kcal/mol above **10**. Because the intermediate **10** already gained some excess energy and the reaction occurs at high temperatures, this barrier can be overcome. We also hope that the intermediate **10**, which is more stable than the product P (**12**) may be detected in the future.

Because it is conceivable that intermediate **10** reacts with $SiCl_4$ to form a chain molecule $Si_3O_2Cl_8$ under elimination of Cl_2, we also calculated the barrier for this process. We found a barrier that is a few kilocalories per mole lower than the one for the ring formation. Thus, it is possible that the chain and ring formation are competing processes.

3.2. Pathway B. In the second reaction scheme, we have considered the unimolecular decomposition of the intermediate Cl_3SiO_2Cl **(3)** into doublet Cl_3SiO and doublet OCl **(13)**, shown in Figures 2 and 4. The barrier for the formation of the two radicals Cl_3SiO and OCl lies 59.5 kcal/mol with respect to the reactants **1** and 11.4 and 30.1 kcal/mol relative to the intermediate Cl_3SiO_2Cl in triplet and singlet states, respectively. Further, Cl_3SiO and OCl each reacts themselves to form the intermediates $(Cl_3SiO)_2$ and O_2Cl_2 **(14)** in the singlet state; the dimerization takes place without any barrier. The intermediate **(14)** lies 50.9 kcal/mol above **1** and 8.6 kcal/mol below **13**. The calculated O−Cl bond length of OCl **(13)** (1.626 Å) is in good agreement with the experimental value of 1.5696 Å.[41] The geometry of O_2Cl_2 **(14)** is shown in Figure 2; the calculated bond lengths O−Cl and O−O, using B3LYP/6-311G*, are 1.856 and 1.295 Å, while the corresponding experimental values are 1.7044 and 1.4259 Å,[42] respectively. B3LYP/6-311G* overestimates the O−Cl bond length by 0.16 Å and underestimate the O−O bond length by 0.13 Å in comparison to the experimental value.[42] The same trend has been observed in a recent calculation using different functionals and extended basis sets.[43] From experimental data[38,44,45] quoted in this paper, it is apparent that our calculations underestimate the O−Cl bond strength and overestimate the O−O bond strength. However, this deviation has no substantial effect on the reaction mechanism. From intermediate **14**, the elimination of Cl_2 to form O_2 involves a transition structure **16**, which lies 92.8 kcal/mol above **1** and 41.9 kcal/mol above **14**. The transition structure **16** calculated in the singlet state joins the intermediates **14** and **18** (Figures 2 and 4).

Considering another possibility, we calculated the dissociation of O_2Cl_2 into radical O_2Cl (**15**) and Cl, which lies 59.6 kcal/mol higher than **1** and 8.7 kcal/mol above **14**. Subsequently, the further dissociation of O_2Cl into O_2 and Cl lies 64.2 kcal/mol relative to **1** and 4.6 kcal/mol to **15**. The dissociation of O_2Cl_2 into O_2Cl and Cl and O_2Cl into O_2 and Cl has been proposed by Molina and Molina[46] for the formation of O_2 from self-reaction of OCl considering a catalytic reaction cycle. From experimental data,[38,44,45] a value of 19 kcal/mol for the dissociation of O_2Cl_2 into $O_2Cl + Cl$ was reported.[43] The reaction path from **14** to **17** passing through **15** is found to be the lowest path for the reaction to proceed further. It involves a total barrier of 13.3 kcal/mol. Structure **17** further stabilizes with the formation of intermediate $(Cl_3SiO)_2 + O_2 + Cl_2$ (**18**), which lies 18.2 kcal/mol above **1** and 46.0 kcal/mol below **17**. The intermediate **18** shown in Figure 2 is found to be minimum on the potential energy surface, and it exists in the trans form.

Our calculated dissociation energy of O_2Cl_2 into $O_2Cl + Cl$ (8.7 kcal/mol) is underestimated in comparison to the experimental value by 10.3 kcal/mol. With the B3LYP/6-311+G(2df) basis set,[42] the dissociation energy was calculated to be 17 kcal/mol, which is in good agreement with the experimental value. However, our B3LYP/6-311G* calculated dissociation energy of O_2Cl into $O_2 + Cl$, 4.6 kcal/mol, is in excellent agreement with the experimentally observed value of 4.83 ± 0.05 kcal/mol,[47] and the B3LYP/6-311+G(2df) calculated value is found

to be 3.8 kcal/mol.[43] It seems that the discrepancy in the case of O_2Cl_2 is basis-set-dependent. Thus, if we also consider the experimental value 19 kcal/mol for the dissociation of O_2Cl_2 into O_2Cl and Cl, the total barrier from **14** to **17** comes out to be 23.6 kcal/mol, which is 10.3 kcal/mol higher than our calculated value.

From intermediate **18**, two channels are available for the formation of the final product $(Cl_2SiO)_2$ (**12**). First, the transfer of a Cl atom from a $SiCl_3$ unit of $(Cl_3SiO)_2$ (**18**) to one of the oxygen atom involves a transition state **19**, which lies 72.7 kcal/mol higher than **1**. We have repeated the calculation of this barrier with the 6-311+G(2df) basis set. The relative energy of **19** to **1** changed to 75.9 kcal/mol, thus retaining the mechanistic relevance. The transition state **19** (Figure 2) shows that the Cl atom is weakly bound to a Si atom with a bond length of 2.558 Å. It starts to join with an oxygen atom to having bond length 2.348 Å, while the O−O bond increased to 1.959 Å compared to 1.475 Å in **18** (Figure 2). The transition state **19** links the intermediates **18** and **9**. Formation of the final product involves the same route as discussed in section 3.1.

In the second pathway, we searched the relative stability of the trans and cis isomers of **18** by rotating the Cl_3SiO unit along the O−O bond. It has been found that these two isomers are separated by a transition state **20**, which lies 34.6 kcal/mol above **1** (Figure 4). We fully optimized the transition state **20**. The calculation of vibrational frequencies produced one negative frequency (Table 1). The structural parameters of **20** are shown in Figure 2. The cis isomer is found to be stable by about 0.4 kcal/mol with respect to **20** with a dihedral angle SiOOSi of about 5.0°.

The dissociation of the cis isomer of **20** into two doublet Cl_3SiO (**21**) needs 27.0 kcal/mol energy with respect to **20** and lies 61.6 kcal/mol with respect to **1**. The formation of Cl_3SiO in **13** and **21** almost lies at the same energy level with a difference of 2.1 kcal/mol. We further calculated the dissociation of Cl_3SiO (**21**) into singlet Cl_2SiO + Cl (**22**), which lies at a relatively high energy of 104.8 kcal/mol from **1** and constitutes a barrier of 43.2 kcal/mol with respect to **21**. Zachariah and Tsang[48] performed ab initio calculations on the reaction of silicon oxyhydride species, $Si_xH_yO_z$. They found an activation energy of 105 kJ/mol (25 kcal/mol) for the dissociation of H_3SiO into H_2SiO and H. From **22**, the formation of the final product P (**12**) proceeds without any barrier. Dimerization of Cl_2SiO into $(Cl_2SiO)_2$ without any barrier has been studied by us earlier,[25] and the similar feature has been observed by Kudo and Nagase[49] for the formation of $(H_2SiO)_2$ from the dimerization of H_2SiO.

Further, the elimination of Cl_2 from the dimer of Cl_3SiO (**21**) leads to the final product **12** via a transition structure **23**, which represents a high barrier of 116.9 kcal/mol from **1** linking **21** and **12**. The structure of **23** is shown in Figure 2. The two oxygen atoms are separated by 2.716 Å, and the two Cl_3SiO units are bent along the O−O bond to form a nonplanar $(SiO)_2$ ring.

An important aspect related to the involvement of certain species responsible for the formation of large chlorosiloxanes is still not clear. The proposed Cl_2SiO was only detected by matrix IR spectroscopy.[23] However, during the reaction of SiH_4 + O_2, H_3SiO was detected as a direct product by the time-resolved mass spectrometry.[18] In our present reaction scheme, the involvement of Cl_3SiO seems to be more favorable over Cl_2SiO for the following reasons: (i) the formation of Cl_3SiO is feasible because it has a comparably low energy barrier (61.6 kcal/mol), while Cl_2SiO involves a relatively high barrier of 104.8 kcal/mol (Figure 4), (ii) the formation of the Cl_3SiO radical is more stable than Cl_2SiO, which is clearly evident from the dissociation energy of Cl_3SiO into Cl_2SiO + Cl (Table 3), and (iii) we further investigated the reaction of Cl_2SiO and Cl_3SiO with $SiCl_4$ for the formation of Cl_6Si_2O using B3LYP/6-311G*. The reaction of Cl_2SiO proceeds through the migration of Cl from $SiCl_4$ to Cl_2SiO, and it involves a barrier of 3.7 kcal/mol. The reaction of Cl_3SiO with $SiCl_4$ proceeds through the abstraction of Cl atom from $SiCl_4$, and it involves a barrier of 4.8 kcal/mol.[50]

3.3. Pathway C. In this reaction scheme, we first considered the dissociation of $SiCl_4$ into $SiCl_3$ and Cl and further its reaction with O_2 as proposed by Hartmann[12] and Britten.[13] We calculated the dissociation energy of $SiCl_4$ into doublet $SiCl_3$ and Cl (**24**) as 95.6 kcal/mol (Figure 5) relative to **1**. It is in good agreement with the experimental reaction enthalpy of 94.1 kcal/mol.[46] However, our earlier calculated value using MP2/6-311+G(2d) was 107.5 kcal/mol,[29] whereas Schlegel et al.[51] calculated the reaction enthalpy value 112 kcal/mol. Using laser flash photolysis of $SiCl_4$, Kunz and Roth[52] measured 110.4 kcal/mol for the abstraction of Cl atom from $SiCl_4$. The other possibilities of abstracting two and three Cl atoms from $SiCl_4$ need relatively high energies of 176.1 and 225.3 kcal/mol,[50] respectively. Our calculated Si−Cl bond length of $SiCl_3$, 2.071 Å, is slightly larger than the experimentally observed value of 2.02 Å.[46] $SiCl_3$ reacts with O_2 to form the Cl_3SiO_2 adduct **5** without any barrier and lies 55.3 kcal/mol higher than **1**. This reaction has been experimentally confirmed because of the fast reaction rate constant of $SiCl_3$ with O_2.[16] The formation of Cl_3SiO_2 (**5**) further stabilizes in **18** with the formation of $(Cl_3SiO)_2$, which follows the same reaction path for the formation of final product **12** as we discussed in section 3.2.

The reaction pathways A and B are displayed in Figure 6 as a diagram, connecting the structures in the sequence in which they are passed through. The structure numbers and their types are also displayed. From Figure 6, it can be easily understood how the reaction is proceeding. For example, up to **3**, both reaction schemes adopt the same route, and from **3**, two energetically favorable paths are available through **4** and **13**, and after passing different points in a sequence, they adopt a common path at **9** for the formation of the final product **12**. The reaction sequence appearing in pathway C (Figure 5) is not shown in Figure 6. We consider it as a special case because the linking of points **5** and **18** can only be achieved by the formation of the $SiCl_3$ radical (Figure 5). Compared to pathways A and B, the formation of $SiCl_3$ is unlikely, because it involves a relatively high energy of 95.7 kcal/mol (Figure 5), while the maximum barriers leading to the minimum energy path in pathways A and B are 76.0 and 72.7 kcal/mol, respectively.

4. Conclusions

In the present study, we have concluded that the insertion of O_2 with $SiCl_4$ occurs in the triplet state involving a relatively low barrier in comparison to the decomposition of $SiCl_4$ into $SiCl_3$ + Cl, which can be easily overcome at high temperatures. We found that the cyclic-Cl_2SiO_2 + Cl_2 channel is the main pathway for the bimolecular reaction with $SiCl_4$. The study proposed the occurrence of an intermediate, $Cl_2SiO(OCl)SiCl_3$ (**10**), more stable than the product, $(Cl_2SiO)_2$ (**12**), as a step before the product formation. The radical Cl_3SiO has been found to be considerably more stable than Cl_2SiO + Cl. Thus, the involvement of Cl_3SiO should be favored over Cl_2SiO in the formation process of larger chlorosiloxanes. The formation of the $SiCl_3$ radical from $SiCl_4$ involves such a high barrier that its occurrence during the reaction is rather unlikely.

Acknowledgment. This research was partially supported by Deutsche Forschungsgemeinschaft. The calculations were performed on the Siemens-Nixdorf VP300 at RRZN Hannover. We thank Prof. M. Binnewies for frequent discussions on the experiments and Prof. H. Willner for information on chlorine−oxygen compounds.

References and Notes

(1) Coltrin, M. E.; Kee, J.; Miller, J. A. *J. Electrochem. Soc.* **1984**, *131*, 425.
(2) Breiland, W. G.; Coltrin, M. E.; Ho, P. *J. Chem. Phys.* **1986**, *59*, 3267.
(3) Jasinski, J. M.; Meyerson, B. S.; Scott, B. A. *Annu. Rev. Phys. Chem.* **1987**, *38*, 109.
(4) Chiang, C.-M.; Zegarski, B. R.; Dubois, L. H. *J. Phys. Chem.* **1993**, *97*, 6948.
(5) Binnewies, M.; Jerzembeck, M.; Kornick, A. *Angew. Chem.* **1991**, *103*, 762.
(6) Binnewies, M.; Jug, K. *Eur. J. Inorg. Chem.* **2000**, 1127.
(7) Binnewies, M.; Jerzembeck, M.; Wilkening, A. *Z. Anorg. Allg. Chem.* **1997**, *263*, 1875.
(8) Kornick, A.; Binnewies, M. *Z. Anorg. Allg. Chem.* **1990**, *587*, 157.
(9) Airey, W.; Glidewell, C.; Robiette, A. G.; Sheldrick, G. M. *J. Mol. Struct.* **1971**, *8*, 413.
(10) Wannagat, U.; Bogedain, C.; Schwarz, A.; Marsmann, H. C.; Brauer, D. J.; Bürger, H.; Dörrenbach, J.; Pawelke, G.; Krüger, C.; Claus, K.-H. *Z. Naturforsch.* **1991**, *46b*, 931.
(11) Törnroos, K. W.; Calzaferri, G.; Imhof, R. *Acta Crystallogr., Sect. C: Cryst. Struct. Commun.* **1995**, *51*, 1732.
(12) Hartmann, J. R.; Famil-Ghiriha, J.; Ring, M. A.; O'Neal, H. E. *Combust. Flame* **1987**, *68*, 43.
(13) Britten, J. A.; Tong, J.; Westbrook, C. K. *Proceedings of the 23rd International Symposium on Combustion*; The Combustion Institute: Orleans, France, 1990; p 195.
(14) Powers, D. R. *J. Am. Ceram. Soc.* **1978**, *61*, 295.
(15) French, W. G.; Pace, L. J.; Foertmeyer, V. A. *J. Phys. Chem.* **1978**, *82*, 2191.
(16) Niiranen, J. T.; Gutman, D. *J. Phys. Chem.* **1993**, *97*, 4106.
(17) Tezaki, A.; Morita, K.; Matsui, H. *J. Phys. Chem.* **1994**, *98*, 10529.
(18) Koshi, M.; Miyoshi, A.; Matsui, H. *J. Phys. Chem.* **1991**, *95*, 9869.
(19) Darling, C. L.; Schlegel, H. B. *J. Phys. Chem.* **1994**, *98*, 8910.
(20) Murakami, Y.; Koshi, M.; Matsui, H.; Kamiya, K.; Umeyama, H. *J. Phys. Chem.* **1996**, *100*, 17501.
(21) Wood, D. L.; Macchesney, J. B.; Luongo, J. P. *J. Mater. Sci.* **1978**, *13*, 2191.
(22) Kornick, A.; Binnewies, M. *Z. Anorg. Allg. Chem.* **1990**, *587*, 167.
(23) Junker, M.; Wilkening, A.; Binnewies, M.; Schnöckel, H. *Eur. J. Inorg. Chem.* **1999**, 1531.
(24) Wilkening, A.; Binnewies, M. *Z. Naturforsch.* **2000**, *55b*, 21.
(25) Jug, K.; Wichmann, D. *J. Mol. Struct. (THEOCHEM)* **1994**, *313*, 155.
(26) Jug, K.; Wichmann, D. *J. Mol. Struct. (THEOCHEM)* **1997**, *398*−*399*, 365.
(27) Wichmann, D.; Jug, K. *J. Phys. Chem. B* **1999**, *103*, 10087.
(28) Jug, K.; Wichmann, D. *J. Comput. Chem.* **2000**, *21*, 1549.
(29) Wichmann, D.; Jug, K. *Chem. Phys.* **1998**, *236*, 87.
(30) Frisch, M. J.; Trucks, G. W.; Schlegel, H. B.; Gill, P. M. W.; Johnson, B. G.; Robb, M. A.; Cheeseman, J. R.; Keith, T.; Petersson, G. A.; Montgomery, J. A.; Raghavachari, K.; Al-Laham, M. A.; Zakrzewski, V. G.; Ortiz, J. V.; Foresman, J. B.; Cioslowski, J.; Stefanov, B. B.; Nanayakkara, A.; Challacombe, M.; Peng, C. Y.; Ayala, P. Y.; Chen, W.; Wong, M. W.; Andres, J. L.; Replogle, E. S.; Gomperts, R.; Martin, R. L.; Fox, D. J.; Binkley, J. S.; Defrees, D. J.; Baker, J.; Stewart, J. P.; Head-Gordon, M.; Gonzalez, C.; Pople, J. A. *Gaussian 94*, revision D.2; Gaussian, Inc.: Pittsburgh, PA, 1995.
(31) Becke, A. D. *Phys. Rev. A* **1988**, *38*, 3098.
(32) Lee, C.; Yang, W.; Parr, R. G. *Phys. Rev. B* **1988**, *37*, 785.
(33) Foresman, J. B.; Frisch, A. *Exploring Chemistry with Electronic Structure Methods*, 2nd ed.; Gaussian, Inc.: Pittsburgh, 1996; p 144 ff.
(34) Gonzalez, C.; Schlegel, H. B. *J. Chem. Phys.* **1990**, *94*, 5523.
(35) Lide, D. R. *Handbook of Chemistry and Physics*, 71st ed.; CRC Press: Boca Raton, FL, 1990.
(36) Zhang, X.; Ding, Y.; Li, Z.; Huang, X.; Sun, C. *Phys. Chem. Chem. Phys.* **2001**, *3*, 965.
(37) Gutsev, G. L. *J. Phys. Chem.* **1994**, *98*, 1570.
(38) Chase, M. W.; Davies, C. A.; Downey, J. R.; Fruriep, D. J.; McDonald, R. A.; Syverud, A. N. JANAF Thermochemical Tables. *J. Phys. Chem. Ref. Data* **1985**, *14* (Suppl. 1).
(39) Kondo, S.; Tokuhashi, K.; Nagai, H.; Takahashi, A.; Aoyagi, M.; Mogi, K.; Minamino, S. *J. Phys. Chem. A* **1997**, *101*, 6015.
(40) Sandhu, V.; Jodhan, A.; Safarik, I.; Strausz, O. P.; Bell, T. N. *Chem. Phys. Lett.* **1987**, *135*, 260.
(41) Leonard, C.; Quere, F. L.; Rosmus, P.; Puzzarini, C.; Castells, M. P. de L. *Phys. Chem. Chem. Phys.* **2000**, *2*, 1117.
(42) Birk, M.; Friedl, R. R.; Cohen, E. A.; Pickett, H. M.; Sander, S. P. *J. Chem. Phys.* **1989**, *91*, 6588.
(43) Fängström, T.; Edvardsson, D.; Ericsson, M.; Lunell, S.; Enkvist, C. *Int. J. Quantum Chem.* **1998**, *66*, 203.
(44) Basco, N.; Hunt, J. E. *Int. J. Chem. Kinet.* **1979**, *11*, 649.
(45) Cox, R. A.; Hayman, G. D. *Nature* **1988**, *332*, 796.
(46) Molina, L. T.; Molina, M. J. *J. Phys. Chem.* **1987**, *91*, 433.
(47) Baer, S.; Hippler, H.; Rahn, R.; Siefke, M.; Seitzinger, N.; Troe, J. *J. Chem. Phys.* **1991**, *95*, 6463.
(48) Zachariah, M. R.; Tsang, W. *J. Phys. Chem.* **1995**, *99*, 5308.
(49) Kudo, T.; Nagase, S. *J. Am. Chem. Soc.* **1985**, *107*, 2589.
(50) Kumar, A.; Jug, K. Unpublished results.
(51) Su, M.-D.; Schlegel, H. B. *J. Phys. Chem.* **1993**, *97*, 9981.
(52) Kunz, A.; Roth, P. *J. Phys. Chem.* **1999**, *103*, 841.